2010 IEEE International Conference on Robotics and Automation
Anchorage Convention District
May 3-8, 2010, Anchorage, Alaska, USA

Spring Loaded Inverted Pendulum Embedding: Extensions toward the Control of Compliant Running Robots

Ioannis Poulakakis

Abstract— **This paper explores systematic control strategies for the stabilization of running on compliant robots with nontrivial torso pitch dynamics. The Spring Loaded Inverted Pendulum (SLIP) embedding controller is revisited and its pertinence to more general legged robot models is investigated. It is first deduced that—in the context of an asymmetric hopper—the existence of a SLIP embedding control law requires nominal running motions in which the torso is kept at a constant angle. To remove this overly restrictive condition, a new method is proposed here that retains the advantage of generating control inputs acting *in concert* with the compliant dynamics of the plant without explicit reliance on the SLIP. To illustrate the enhanced control authority afforded by the proposed method, a minimalist setting is considered, in which a three-degree-of-freedom asymmetric hopper is controlled by a *single* actuator located at the hip.**

I. Introduction

Dynamically stable legged robots like the monopod Thumper portrayed in Fig. 1(a) pose unique challenges to existing nonlinear control synthesis tools. The hybrid and underactuated nature of such systems, combined with the multitude of constraints that must be respected by the control action—including actuator and ground contact limitations—posit the need for developing control laws that work harmoniously with the open-loop plant dynamics in inducing stable running motions on these robots.

To resolve complexity, the idea of task encoding through the enforcement of a lower-dimensional target dynamics—rather than through the prescription of a set of reference trajectories—has been employed in the relevant literature. In the light of evidence in biomechanics, [3], and robotics, [10], the Spring Loaded Inverted Pendulum (SLIP) has been proposed as a canonical model of the center-of-mass dynamics in running, and studied extensively as a target for control in animals—see [3] and references therein—and robots—see [11] and [1].

Along these lines, the *SLIP embedding controller* has been proposed in [9] as a method that combines established nonlinear control synthesis tools, such as the Hybrid Zero Dynamics (HZD) developed in [12], with empirical control procedures obtained in the context of the SLIP, such as those introduced by Raibert in [10], to induce provably exponentially stable running motions in an asymmetric compliant hopper termed the *Asymmetric Spring Loaded Inverted Pendulum* (ASLIP); see Fig. 1(b). The SLIP embedding controller generates corrective action that works together

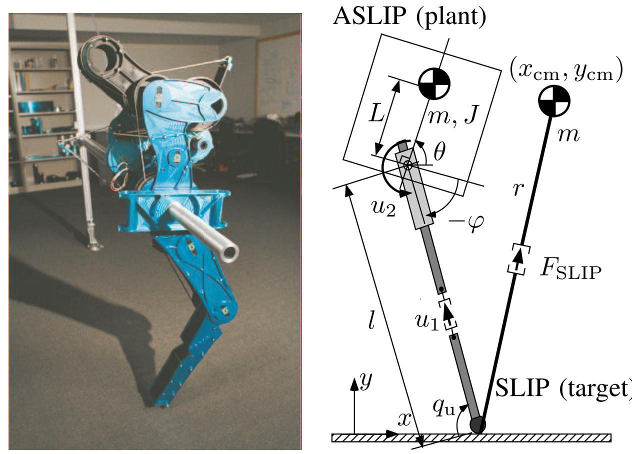

(a) (b)

Fig. 1. (a) Thumper (courtesy of Prof. J. W. Hurst); see [4] for design details. Note that the hip joint does *not* coincide with the torso's center of mass. (b) The Asymmetric Spring Loaded Inverted Pendulum (ASLIP) introduced in [9] is a more faithful representation of Thumper than point-mass hoppers. In [9], the leg force u_1 was modeled as a spring in parallel with a prismatic force source; in Section IV below, u_1 corresponds to a passive spring. In the SLIP embedding controller, the COM of the SLIP $(x_{\rm cm}, y_{\rm cm})$ coincides with that of the ASLIP, see [9, Fig. 1].

with compliance allowing for large perturbations to be accommodated, with small actuator effort and without violation of the unilateral constraints between the toe and the ground. Other controllers that have been proposed in the literature for asymmetric hoppers similar to the ASLIP include [5], and [6], in which rough terrain locomotion is also addressed.

In this paper, we turn our attention to investigating the potential implementation of SLIP embedding in more general settings. First, an intuitive explanation of how the SLIP embedding controller utilizes compliance to generate inputs that respect the plant's natural dynamics is provided. It is this property, combined with the constructive nature of the method, that renders SLIP embedding an attractive alternative to existing heuristic control procedures for legged robots. However, as is shown in this paper, a *necessary* condition for its implementation in the context of the ASLIP is the existence of nominal running gaits in which the torso remains constant. The fact that this requirement excludes a large variety of motions where the torso is allowed to oscillate—such motions are inevitably present in robots like Thumper—calls for a more general method. Proposing such a method that preserves the advantages of SLIP embedding, yet removes the requirement for explicit reliance on the SLIP is at the core of this work. It is anticipated that the generality of the proposed approach, which is independent of the particular

I. Poulakakis is with the Department of Mechanical and Aerospace Engineering, Princeton University, Princeton, NJ 08544-5263, U.S.A. Phone: +1-609-258-0303; fax: +1-609-258-6109; e-mail: poulakas@princeton.edu.

mathematical structure that permitted exact SLIP embedding, will be of use to the control of more complete robot models.

II. Overview of the Method

As enunciated by Raibert, [10], the control objectives for monopedal running can be decomposed into the regulation of three key variables: torso angle, hopping height, and forward velocity. Following the control paradigm of [12], these control objectives are encoded in a set of suitably designed constraints that are imposed on the system's dynamics in continuous time through its actuators. These constraints, suitably parameterized, can be interpreted as *(virtual) holonomic constraints*, which restrict the dynamics on lower-dimensional surfaces embedded in the state spaces of the continuous-time phases. Loosely speaking, this *reduction-by-feedback* procedure effectively reduces the feasible motions of the system by *coordinating* its actuated degrees of freedom, so that a lower-dimensional hybrid subsystem "emerges" from the robot's closed-loop dynamics. This lower-dimensional hybrid subsystem governs the existence and stability properties of distinguished periodic orbits that correspond to running motions of interest.

To achieve such coordination, the feedback law exploits the hybrid nature of the system by introducing control action in continuous-time within the stance phase and in discrete time by updating controller parameters at transitions between the stance and flight phases; see Fig. 2. In the remainder of this section, the general procedure of how to design the continuous and discrete time control laws is highlighted.

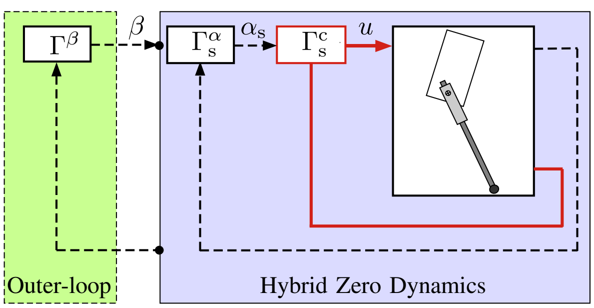

Fig. 2. Feedback diagram presenting the basic structure of the controller. Continuous lines represent signals in continuous time; dashed lines represent signals in discrete time.The control laws $\Gamma_{\rm s}^{\rm c}$ and $\Gamma_{\rm s}^{\alpha}$ are intended to create a well defined hybrid zero dynamics (HZD), while the controller Γ^{β} ensures that the resulting HZD is exponentially stable.

A. ASLIP Open-loop Hybrid Dynamics

The ASLIP hybrid dynamics, combining the stance and flight phases with the discrete transitions between them, can be written in the form of a system with impulse effects, [12],

$$\Sigma^{\rm ASLIP} : \begin{cases} \dot{x}_{\rm s} = f_{\rm s}(x_{\rm s}) + g_{\rm s}(x_{\rm s})u, & x_{\rm s}^{-} \notin \mathcal{S}_{\rm s\to f} \\ x_{\rm s}^{+} = \Delta\left(x_{\rm s}^{-}, \beta_{\rm f}\right), & x_{\rm s}^{-} \in \mathcal{S}_{\rm s\to f}, \end{cases} \tag{1}$$

in which the continuous part corresponds to the stance dynamics parameterized by the configuration variables: leg length l, leg angle φ, and torso angle θ, i.e., $q_{\rm s} = (l, \varphi, \theta)$; see Fig. 1(b). In (1), Δ is the map taking the state $x_{\rm s}^{-}$ just prior to liftoff to the state $x_{\rm s}^{+}$ just after touchdown, $\mathcal{S}_{\rm s\to f}$ is the stance to flight switching surface, and $\beta_{\rm f} = (l^{\rm td}, \varphi^{\rm td})$ are the touchdown parameters—leg length and angle—which do not trigger stance to flight switching, but influence the termination of the flight phase, thus affecting the initial conditions $x_{\rm s}^{+}$ of the stance phase. Detailed descriptions of the components of (1) can be found in [9, Section III].

B. In-Stride Continuous-Time Control

To the continuous-time dynamics of the stance phase in (1) associate the output

$$y = h(q_{\rm s}, \alpha_{\rm s}, \beta_{\rm s}) := q_{\rm c} - h_{\rm d}\left(q_{\rm u}(q_{\rm s}), \alpha_{\rm s}, \beta_{\rm s}\right), \tag{2}$$

where $q_{\rm c}$ contains the *controlled* variables and $h_{\rm d}$ is the desired evolution parameterized by $q_{\rm u}$, a strictly monotonic (increasing) quantity that is a function of the generalized coordinates $q_{\rm s}$. The parameter arrays $\alpha_{\rm s}$ and $\beta_{\rm s}$ in general include coefficients of polynomials representing the virtual constraints; their precise meaning will be discussed below.

For given $\alpha_{\rm s}$ and $\beta_{\rm s}$, differentiating (2) twice with respect to time results in

$$\frac{d^2y}{dt^2} = L_{f_{\rm s}}^2 h(x_{\rm s}, \alpha_{\rm s}, \beta_{\rm s}) + L_{g_{\rm s}} L_{f_{\rm s}} h(q_{\rm s}, \alpha_{\rm s}, \beta_{\rm s})u, \tag{3}$$

and, if $L_{g_{\rm s}} L_{f_{\rm s}} h(q_{\rm s}, \alpha_{\rm s}, \beta_{\rm s})$ is invertible,

$$u^*(x_{\rm s}, \alpha_{\rm s}, \beta_{\rm s}) = -\left(L_{g_{\rm s}} L_{f_{\rm s}} h(q_{\rm s}, \alpha_{\rm s}, \beta_{\rm s})\right)^{-1} L_{f_{\rm s}}^2 h(x_{\rm s}, \alpha_{\rm s}, \beta_{\rm s}) \tag{4}$$

is the unique input that renders the zero dynamics surface

$$\mathcal{Z}_{(\alpha_{\rm s}, \beta_{\rm s})} = \{x_{\rm s} \in TQ_{\rm s} \mid h(q_{\rm s}, \alpha_{\rm s}, \beta_{\rm s}) = 0, \quad L_{f_{\rm s}} h(x_{\rm s}, \alpha_{\rm s}, \beta_{\rm s}) = 0\} \tag{5}$$

invariant under the flow of the continuous part of the ASLIP dynamics, that is, for every $z \in \mathcal{Z}_{(\alpha_{\rm s}, \beta_{\rm s})}$

$$f^*(z, \alpha_{\rm s}, \beta_{\rm s}) = f_{\rm s}(z) + g_{\rm s}(z)u^*(z, \alpha_{\rm s}, \beta_{\rm s}) \in T_z\mathcal{Z}_{(\alpha_{\rm s}, \beta_{\rm s})}.$$

The restriction of f^* on the surface $\mathcal{Z}_{(\alpha_{\rm s}, \beta_{\rm s})}$, i.e.

$$\dot{z} = f^*|_{\mathcal{Z}_{(\alpha_{\rm s}, \beta_{\rm s})}}(z, \alpha_{\rm s}, \beta_{\rm s}), \tag{6}$$

is the stance phase zero dynamics of the ASLIP, which depends on the coefficients $\alpha_{\rm s}$ and $\beta_{\rm s}$. Finally, to establish attractivity of $\mathcal{Z}_{(\alpha_{\rm s}, \beta_{\rm s})}$, the input (4) is modified as:

$$\begin{aligned} u &= \Gamma_{\rm s}^{\rm c}(x_{\rm s}, \alpha_{\rm s}, \beta_{\rm s}) \\ &= \left(L_{g_{\rm s}} L_{f_{\rm s}} h(q_{\rm s}, \alpha_{\rm s}, \beta_{\rm s})\right)^{-1} [\upsilon(y, \dot{y}, \epsilon) - L_{f_{\rm s}}^2 h(x_{\rm s}, \alpha_{\rm s}, \beta_{\rm s})], \end{aligned} \tag{7}$$

where $\upsilon(y, \dot{y}, \epsilon) = -(1/\epsilon^2)K_{\rm P}y - (1/\epsilon)K_{\rm V}\dot{y}$ and $K_{\rm P}$, $K_{\rm V}$ positive gains and $\epsilon > 0$.

C. Event-Based Discrete-Time Control

The continuous-time controller of Section II-B introduced a set of parameters $\alpha_{\rm s}$ and $\beta_{\rm s}$, which, together with the flight parameters $\beta_{\rm f}$, can be updated at transitions between continuous phases. The division of the stance parameters in the two arrays $\alpha_{\rm s}$ and $\beta_{\rm s}$ follows the structure of the event-based parameter update law, which is organized in an inner/outer-loop architecture. The inner-loop controller

$$\alpha_{\rm s}^{+} = \Gamma_{\rm s}^{\alpha}(x_{\rm s}^{+}) \tag{8}$$

updates the parameters α_s to ensure that the initial condition x_s^+ of the stance phase lies on the surface $\mathcal{Z}_{(\alpha_s,\beta_s)}$. Intuitively, updating α_s affects the "entry" conditions to the stance phase, by locally deforming $\mathcal{Z}_{(\alpha_s,\beta_s)}$ so that $x_s^+ \in \mathcal{Z}_{(\alpha_s,\beta_s)}$. This inner-loop controller leads to the creation of a reduced-order hybrid subsystem

$$\Sigma_{\text{HZD}}^{\text{ASLIP}}: \begin{cases} \begin{bmatrix} \dot{z} \\ \dot{\beta}_s \end{bmatrix} = \begin{bmatrix} f^*|_{\mathcal{Z}_{(\alpha_s,\beta_s)}}(z,\beta_s) \\ 0 \end{bmatrix}, \\ \qquad\qquad z^- \notin \mathcal{S}_{s\to f} \cap \mathcal{Z}_{(\alpha_s,\beta_s)} \\ \begin{bmatrix} z^+ \\ \beta^+ \end{bmatrix} = \begin{bmatrix} \Delta(z^-,\beta_f) \\ \Gamma^\beta(z^-) \end{bmatrix}, \\ \qquad\qquad z^- \in \mathcal{S}_{s\to f} \cap \mathcal{Z}_{(\alpha_s,\beta_s)}, \end{cases} \tag{9}$$

which is the *Hybrid Zero Dynamics* (HZD) associated with the output (2), and it governs the stability properties of the full-order ASLIP; [12]. A *critical* aspect of (9) is its dependence on the parameter array $\beta = \{\beta_s, \beta_f\}$, which can be selected according to an outer-loop feedback law Γ^β, whose purpose is to exponentially stabilize (9). One way of designing Γ^β would be to use Raibert's intuitive control procedures in [10]. An alternative, which will be employed in Section IV-B below, is to use discrete LQR techniques.

III. SLIP Embedding: Benefits and Limitations

The SLIP embedding controller has been proposed in [9] as a first step toward a general framework for designing control laws that stabilize running in compliant robots. The objective of the control action is to impose via feedback enough structure on the system allowing for tractable stability analysis without "destroying" components of the open-loop dynamics—such as compliance—that are important in achieving the task of running. The purpose of this section is to put SLIP embedding in perspective relative to its applicability in controlling running in robots like Thumper, and to motivate the results of Section IV, in which the method is generalized so that its exact dependence on the SLIP, which in general is difficult to implement, is relaxed.

A. SLIP Embedding: Preserving Open-loop Compliance

The SLIP embedding controller achieves the dual objective of working harmoniously with the natural compliant dynamics of the ASLIP and of affording provable stability guarantees by manipulating the control inputs so that, for sufficiently fast exponentially contracting pitch error dynamics, the SLIP emerges as the HZD (9) of the ASLIP. An intuitive explanation of how the control action respects the system's natural dynamics, resulting in the large domains of attraction reported in [9], is given here. As [9, eq. (58)] suggests, under the SLIP embedding controller, the total ASLIP leg force, u_1, becomes equal to the projection of the SLIP spring force, F_{SLIP}, along the direction of the ASLIP leg, that is

$$u_1 = \frac{l - L\sin\varphi}{r} F_{\text{SLIP}} \;\Leftrightarrow\; u_1 = (\cos\chi)\, F_{\text{SLIP}}, \tag{10}$$

where $r = \sqrt{L^2 + l^2 - 2Ll\sin\varphi}$ and the angle χ is shown in Fig. 3. In view of the assumption—see [9, Fig. 1 and eq. (76)]—that the total leg force u_1 corresponds to a spring force $k_A(l_0 - l)$ in parallel with an actuator u_1^a, i.e.

$$u_1 = u_1^a + k_A(l_0 - l), \tag{11}$$

the leg actuator u_1^a is only required to "shape" the actual spring force $k_A(l_0 - l)$, so that u_1 results in the required force F_{SLIP} developed along the virtual (SLIP) leg direction, as (10) dictates. As can be seen in Fig. 3, for physically reasonable torso pitch angles, the angle between the actual leg and the virtual leg direction is small. Consequently, small actuator effort suffices to "shape" the spring force of the actual leg to achieve this projection, thus providing a qualitative explanation of the superiority of the SLIP-embedding controller under transient conditions against controllers that create non-compliant HZD, as reported in [9, Sec. IX].

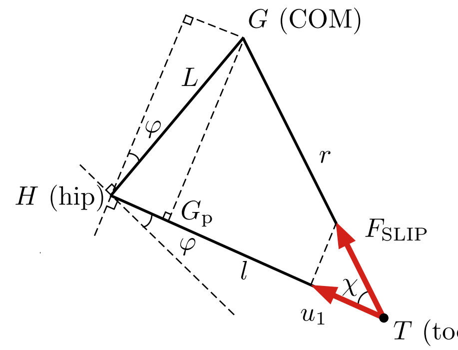

Fig. 3. The SLIP embedding configuration; see [9, Fig. 1] or Fig. 1(b) with the COM of the SLIP coinciding with that of the ASLIP. The leg force u_1 equals the projection of the SLIP force F_{SLIP} along the ASLIP leg.

B. SLIP Embedding: Limitations

The SLIP embedding controller uses the hip torque u_2 according to the procedure of Section II-B—see [9, Sections VI and VII] for details—to stabilize the torso angle θ at a desired *constant* pitch angle $\bar{\theta}$, i.e. $q_c = \theta$ and $h_d(q_s) = \bar{\theta}$ in (2). Hence, the virtual holonomic constraint imposed during stance is a constant polynomial with coefficient $\alpha_{s,0} = \bar{\theta}$. This condition however can be overly restrictive—especially in the case of robots like Thumper with nonzero leg inertia—since a large variety of running motions in which the torso is allowed to move are excluded. It is therefore natural to ask if this condition can be relaxed.

It is shown next that requiring a constant pitch angle during the nominal stance phase is, in fact, a *necessary* condition for the existence of a SLIP embedding control law. In other words, allowing the pitch angle to vary during the nominal stance phase implies that no feedback law exists that will render the COM dynamics of the ASLIP diffeomorphic to the SLIP. To show this statement, the problem is formulated as an output zeroing problem imposed on an extended system, in which the plant is the ASLIP and the target model is the SLIP; see Fig. 1(b). This corresponds to a nonlinear model matching problem; refer to [2] for the relevant background.

The extended system associated with the ASLIP and the SLIP stance dynamics is defined as

$$\dot{x}_s^e = f_s^e(x_s^e) + g_s^e(x_s^e)\, u^e, \tag{12}$$

with state vector $x_{\mathrm{s}}^{\mathrm{e}} := \mathrm{col}\left(q_{\mathrm{s}}^{\mathrm{A}},\ q_{\mathrm{s}}^{\mathrm{S}},\ \dot{q}_{\mathrm{s}}^{\mathrm{A}},\ \dot{q}_{\mathrm{s}}^{\mathrm{S}}\right)$, in which $q_{\mathrm{s}}^{\mathrm{A}} = (l, \varphi, \theta)$ are the ASLIP states and $q_{\mathrm{s}}^{\mathrm{S}} = (x_{\mathrm{cm}}, y_{\mathrm{cm}})$ are the states of the SLIP, and input vector $u_{\mathrm{s}}^{\mathrm{e}} := u$, the inputs of the ASLIP; see Fig. 1(b).

The feedback action generated by the SLIP embedding controller renders the COM dynamics of the ASLIP diffeomorphic to the SLIP dynamics. In the extended system (12), this requirement is equivalent to zeroing the output

$$y = h\left(q_{\mathrm{s}}^{\mathrm{e}}\right) := q_{\mathrm{s}}^{\mathrm{S}} - \bar{h}\left(q_{\mathrm{s}}^{\mathrm{A}}\right), \tag{13}$$

where $\bar{h}\left(q_{\mathrm{s}}^{\mathrm{A}}\right)$ is determined by

$$\bar{h}\left(q_{\mathrm{s}}^{\mathrm{A}}\right) := \begin{bmatrix} -l\sin(\varphi+\theta) + L\cos\theta \\ l\cos(\varphi+\theta) + L\sin\theta \end{bmatrix}; \tag{14}$$

see Fig. 1(b). Geometrically, the output (13)–(14) corresponds to the difference between the Cartesian positions of the COM of a SLIP and an ASLIP with their toes coinciding.

It is of interest to analyze the zero dynamics associated with the output (13)–(14). According to the procedure of Section II-B, the zero dynamics surface is defined by

$$\mathcal{Z}^{\mathrm{e}} := \left\{x_{\mathrm{s}}^{\mathrm{e}} \in TQ_{\mathrm{s}}^{\mathrm{e}} \mid h\left(q_{\mathrm{s}}^{\mathrm{e}}\right) = 0,\ L_{f_{\mathrm{s}}^{\mathrm{e}}} h\left(x_{\mathrm{s}}^{\mathrm{e}}\right) = 0\right\}, \tag{15}$$

and it includes all the states of the extended system in which the COM dynamics of the ASLIP matches exactly the dynamics of the SLIP. The corresponding zero dynamics is computed by restricting on $\mathcal{Z}^{\mathrm{e}}$ the closed-loop system

$$f^*(x_{\mathrm{s}}^{\mathrm{e}}) = f_{\mathrm{s}}^{\mathrm{e}}(x_{\mathrm{s}}^{\mathrm{e}}) + g_{\mathrm{s}}^{\mathrm{e}}(x_{\mathrm{s}}^{\mathrm{e}})u^*(x_{\mathrm{s}}^{\mathrm{e}}), \tag{16}$$

in which the input u^* is computed by (4) as

$$u^*(x_{\mathrm{s}}^{\mathrm{e}}) = -\frac{1}{\sqrt{x_{\mathrm{cm}}^2 + y_{\mathrm{cm}}^2}}\ P(q_{\mathrm{s}}^{\mathrm{e}})\ F_{\mathrm{SLIP}}(q_{\mathrm{s}}^{\mathrm{S}}), \tag{17}$$

where

$$P(q_{\mathrm{s}}^{\mathrm{e}}) = \begin{bmatrix} x_{\mathrm{cm}}\sin(\varphi+\theta) - y_{\mathrm{cm}}\cos(\varphi+\theta) \\ l\left(x_{\mathrm{cm}}\cos(\varphi+\theta) + y_{\mathrm{cm}}\sin(\varphi+\theta)\right) \end{bmatrix}, \tag{18}$$

and $F_{\mathrm{SLIP}}(q_{\mathrm{s}}^{\mathrm{S}}) = k(r_0 - \sqrt{x_{\mathrm{cm}}^2 + y_{\mathrm{cm}}^2})$ is the standard SLIP leg force. To reveal the underlying structure of the zero dynamics associated with the output (13), the coordinates $z = \mathrm{col}(q_{\mathrm{z}}, \dot{q}_{\mathrm{z}})$ with $q_{\mathrm{z}} := \mathrm{col}(q_{\mathrm{s}}^{\mathrm{S}}, \theta)$ are used to parameterize $\mathcal{Z}^{\mathrm{e}}$. Then, the zero dynamics can be computed explicitly, and after some algebraic manipulations is found to be

$$\begin{bmatrix} \ddot{x}_{\mathrm{cm}} \\ \ddot{y}_{\mathrm{cm}} \end{bmatrix} = \begin{bmatrix} \dfrac{1}{m}\dfrac{x_{\mathrm{cm}}}{\sqrt{x_{\mathrm{cm}}^2 + y_{\mathrm{cm}}^2}}\ F_{\mathrm{SLIP}}(q_{\mathrm{s}}^{\mathrm{S}}) \\ \dfrac{1}{m}\dfrac{y_{\mathrm{cm}}}{\sqrt{x_{\mathrm{cm}}^2 + y_{\mathrm{cm}}^2}}\ F_{\mathrm{SLIP}}(q_{\mathrm{s}}^{\mathrm{S}}) - g \end{bmatrix} \tag{19}$$

and

$$\ddot{\theta} = 0. \tag{20}$$

In words, the zero dynamics corresponding to the output (13)–(14) is the combination of two completely decoupled and conservative subsystems. The translational part (19), which can be recognized as the SLIP dynamics in the coordinates $q_{\mathrm{s}}^{\mathrm{S}}$, and the rotational part (20) that governs the pitch dynamics. By the maximality property of the zero dynamics see [7, p. 294], (19) and (20) is the "largest" dynamics compatible with the output (13)–(14) being zero. As a result it can be deduced that, if the translational dynamics of the ASLIP is diffeomorphic to the SLIP stance dynamics, then the pitch velocity *must* be equal to a constant. If this constant is nonzero, then the torso tumbles, i.e. it monotonically rotates during the gait resulting in unrealistic running motions. On the other hand, if the constant is zero, as is assumed to be in the SLIP embedding controller, the torso remains at a desired (upright) posture.

C. Discussion

The SLIP embedding controller provides a systematic way of designing control laws with provable properties for compliant running robot models such the ASLIP. The method, which is detailed in [9], combines constructive nonlinear controller synthesis tools with intuitive control procedures to generate control actions that work together with the open-loop compliance to produce efficient, natural-like running motions. The SLIP embedding controller can be envisioned as a "building block" toward a general control synthesis framework for more elaborate models that constitute more accurate representations of legged robots, such as the monopedal robot Thumper of Fig. 1.

However, implementing the SLIP embedding controller—even in the simplified setting of the ASLIP—requires conditions that may limit its authority in controlling more general robot models. In particular, as was shown in Section III-B, the SLIP embedding controller requires nominal running orbits in which the pitch angle remains constant. This condition may be overly restrictive, since it excludes a large variety of running motions, rendering the method hard, or even impossible, to implement in models that are more complete than the ASLIP. For instance, in legged robots like Thumper, the leg inertia cannot be considered negligible, thus, inevitably resulting in nontrivial torso pitching. In addition, the SLIP embedding controller requires establishing a diffeomorphic equivalence between appropriate restrictions of the robot dynamics and the SLIP. For general systems, providing conditions that guarantee the existence of such coordinate transformations between the COM dynamics of the system and the SLIP can be an intractable problem.

Embedding the SLIP as the HZD of the ASLIP is a rather conservative way of ensuring that the open-loop compliance is preserved under feedback. Evidently, a generalization is required so that the advantage of making efficient use of the spring is retained, while the technical burden of establishing diffeomorphic equivalence between the system's COM dynamics and the SLIP is removed. The development of such method is undertaken in the following section.

IV. Reduction-by-Feedback and Compliant HZD Control of the ASLIP

This section proposes a feedback law for the ASLIP, which generalizes the SLIP embedding controller in the sense that the control action preserves the compliant nature of the open-loop system *without* imposing the SLIP as its COM dynamics. As a result, the torso pitch angle need not be constant, thus providing a much larger family of nominal running orbits, in which the torso is allowed to oscillate. To illustrate the flexibility afforded by relaxing the requirement for exact SLIP embedding, a minimalist control setting is assumed, in which the ASLIP is powered by a *single* actuator located at the hip; no active control is present along the leg, which is assumed to be a passive spring. Hence, contrary to the SLIP embedding controller, u_1^{a} in (11) is zero. The method is developed within the framework of Section II.

A. In-Stride Continuous-Time Control

Following the structure of Fig. 2, a continuous-time feedback law $\Gamma_{\mathrm{s}}^{\mathrm{c}}$ is employed during stance with the purpose of stabilizing the torso and of preparing the system for the upcoming flight phase. The controlled variable q_{c} in (2) is selected to be the torso orientation θ, while h_{d} represents its desired evolution, which will be parameterized with respect to the strictly monotonic (increasing) quantity q_{u} corresponding to the angle of the ASLIP leg with respect to the ground,

$$q_{\mathrm{u}} = \frac{\pi}{2} - \theta - \varphi; \tag{21}$$

see also Fig. 1(b). To ease implementation, it is favorable to use Beziér polynomials to design h_{d}. Let $q_{\mathrm{u}}^{\min}$ and $q_{\mathrm{u}}^{\max}$ be the minimum and maximum values of the angle q_{u} during a nominal stance phase, and define the parameter

$$s = \frac{q_{\mathrm{u}} - q_{\mathrm{u}}^{\min}}{q_{\mathrm{u}}^{\max} - q_{\mathrm{u}}^{\min}}, \tag{22}$$

with $s \in [0, 1]$. Then, the desired evolution h_{d} can be parameterized by the following fourth order Beziér polynomial

$$h_{\mathrm{d}}(s(q_{\mathrm{s}})) = \sum_{k=0}^{2} b_k(s)\alpha_{\mathrm{s},k} + b_3(s)\beta_{\mathrm{s},1} + b_4(s)\beta_{\mathrm{s},2} \tag{23}$$

in which the coefficients b_k, $k \in \{0, ..., 4\}$, are given by

$$b_k(s) := \frac{M!}{k!\ (M-k)!}\ s^k\ (1-s)^{M-k}; \tag{24}$$

and $M = 4$. Enforcing (23) through zeroing the output (2) introduces the surface $\mathcal{Z}_{(\alpha_{\mathrm{s}},\beta_{\mathrm{s}})}$ that depends on the coefficients of the polynomial (23), which are divided in the two arrays α_{s} and β_{s} to distinguish between their different control roles. These different roles are explained here. By properties of the Beziér polynomials,

$$\begin{gathered} h_{\mathrm{d}}(0) = \alpha_{\mathrm{s},0},\ h_{\mathrm{d}}(1) = \beta_{\mathrm{s},2}, \\ \left.\frac{\partial h_{\mathrm{d}}}{\partial s}\right|_{s=0} = M(\alpha_{\mathrm{s},1} - \alpha_{\mathrm{s},0}),\ \left.\frac{\partial h_{\mathrm{d}}}{\partial s}\right|_{s=1} = M(\beta_{\mathrm{s},2} - \beta_{\mathrm{s},1}). \end{gathered} \tag{25}$$

From (25) it is seen that $\alpha_{\mathrm{s},0}$ and $\alpha_{\mathrm{s},1}$ are associated with the *entry* conditions of the stance phase—updating these parameters affects the desired pitch angle and velocity commanded at the beginning of stance—while $\beta_{\mathrm{s},1}$ and $\beta_{\mathrm{s},2}$ are associated with the *exit* conditions—updating these parameters affects the pitch angle and velocity at the end of the stance phase. The parameters $\beta_{\mathrm{s},1}$ and $\beta_{\mathrm{s},2}$ provide a powerful control mechanism for stabilizing the ASLIP.

B. Event-Based Discrete-Time Control

The event-based discrete-time component of the control law updates the parameters α and β at transitions between continuous phases, and it is organized in the inner/outer-loop architecture depicted in Fig. 2. The inner-loop controller $\Gamma_{\mathrm{s}}^{\alpha}$ properly updates α_{s} at touchdown to ensure that the initial condition x_{s}^{+} of the upcoming stance phase lies on the surface $\mathcal{Z}_{(\alpha_{\mathrm{s}},\beta_{\mathrm{s}})}$, i.e., $x_{\mathrm{s}}^{+} \in \mathcal{Z}_{(\alpha_{\mathrm{s}},\beta_{\mathrm{s}})}$. This condition is referred to as *hybrid invariance* and can be achieved through the following rule

$$\alpha_{\mathrm{s},0}^{+} = \theta^{+},\ \alpha_{\mathrm{s},1}^{+} = \frac{\dot{\theta}^{+}}{M\dot{s}^{+}} + \alpha_{\mathrm{s},0}^{+}, \tag{26}$$

as suggested by the properties (25) of Beziér polynomials. The inner-loop controller $\Gamma_{\mathrm{s}}^{\alpha}$ leads to the creation of a well defined HZD, which has the form of (9).

The dependence of the HZD (9) on $\beta = \{\beta_{\mathrm{s}}, \beta_{\mathrm{f}}\}$ allows for further control action. Given the discussion in Section IV-A, β_{s} provides a means for controlling the pitch angle and velocity when the ASLIP enters the flight phase, while the touchdown angle β_{f} provides a powerful control input determining when the flight phase is terminated. Hence, according to the feedback diagram of Fig. 2, the parameters β will be updated at liftoff to render the HZD (9) exponentially stable. This can be done by using intuitive control procedures such as those introduced by Raibert in [10]. An alternative is to use discrete LQR control approaches. Selecting the Poincaré section to be the surface $\mathcal{S}_{\mathrm{s}\to\mathrm{f}}$, the Poincaré map $\mathcal{P}$ associated with the hybrid system (9) gives rise to the discrete-time control system

$$z^{-}[k+1] = \mathcal{P}\left(z^{-}[k], \beta[k]\right). \tag{27}$$

Linearizing (27) and implementing a discrete LQR results in the following rule for updating β

$$\beta^{+} := \beta[k] = \bar{\beta} + K\left(z^{-}[k] - \bar{z}^{-}\right) =: \Gamma^{\beta}(z^{-}), \tag{28}$$

where $\bar{z}^{-}$ is the nominal (fixed-point) value of the restricted state just prior to k-th liftoff, and $\bar{\beta}$ the nominal value of the parameters β. The feedback controller (28) guarantees that all the eigenvalues of the linearization of (27) are within the unit circle, and completes the control design.

C. Simulation Results

The mechanical properties of the ASLIP used in the simulations are those in [9, Table I], and they roughly correspond to the monopedal robot Thumper. Finding a periodic motion for the ASLIP in closed-loop with the controller developed in Sections IV-A and IV-B can be cast as a constrained minimization problem according to the procedure of [12, Ch. 6]. This procedure results in a fixed point of the Poincaré map (27) and in the nominal values of the parameters. Fig. 4 shows the COM evolution in Cartesian space and the torso angle during a nominal (fixed point) gait. The dashed part of Fig. 4(b) corresponds to the stance phase virtual constraint (23). Note that the torso is allowed to oscillate while all the constraints—e.g. actuator limitations, toe/ground interaction constraints—are respected.

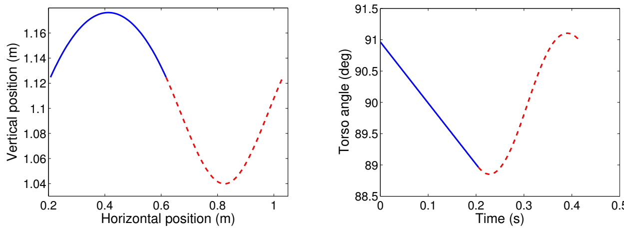

(a) (b)

Fig. 4. Cartesian position of the COM, (a), and torso pitch angle evolution, (b), during a nominal running step. The dashed line represents stance phase.

To illustrate the orbit's local stability, the state prior to liftoff is perturbed away from the fixed point by an initial error of $\delta\theta = +5\mathrm{deg}$ and $\delta\dot{x} = +0.1\mathrm{m/s}$. Figs. 5 and 6 present the evolution of various states and of the input in converging to the nominal orbit. Figs. 5(b) and 5(d) illustrate how the outer-loop controller updates the coefficients β_{s}, corresponding to the torso pitch and pitch rate prior to liftoff. It is the introduction of this component, namely Γ^{β}, in the event-based controller that allows to stabilize the total energy without the need of an extra leg actuator devoted to this purpose, as was the case in the SLIP embedding controller.

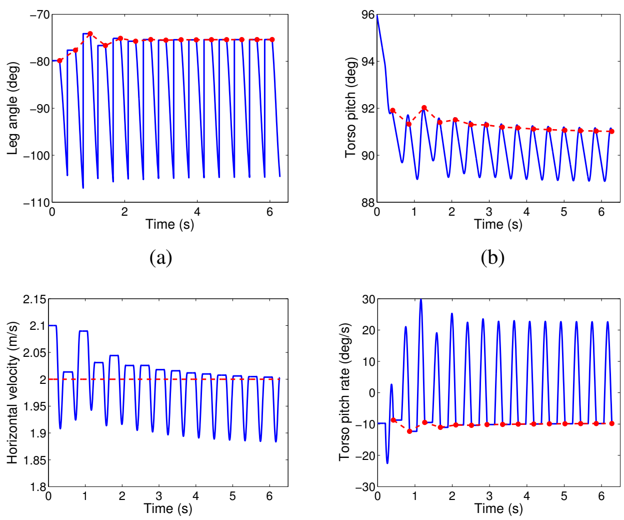

(c) (d)

Fig. 5. Evolution with respect to time showing convergence from a perturbation: leg angle, (a); torso pitch angle, (b); COM horizontal velocity, (c); torso pitch rate, (d). The red circles represent commanded touchdown angle in (a), and commanded liftoff pitch angle in (b) and pitch rate in (d) corresponding to updates of the parameters β by the outer-loop controller Γ^{β} of Fig. 2. The norm of the maximum eigenvalue is 0.8.

V. Conclusion

Motivated by the fact that embedding the SLIP as the HZD of the ASLIP requires running gaits in which the torso remains constant, and given that such motions cannot be imposed on our monopedal robot Thumper, a more general control approach is proposed in this work. This approach preserves the advantage of efficient use of the open-loop spring, while it relaxes the explicit reliance on the SLIP dynamics. The development of the control law is systematic, offering

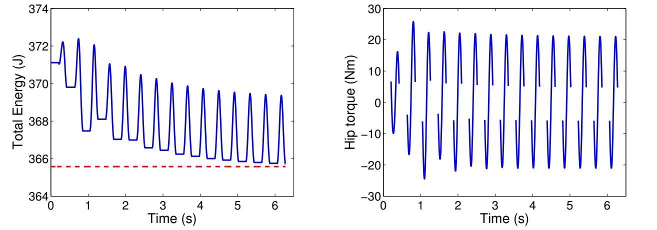

(a) (b)

Fig. 6. Total energy, (a), and hip actuator torque, (b). The dashed line in (a) represents nominal value.

analytical tractability and provable stability properties of the resulting closed-loop system. In addition, it generalizes other HZD controllers [12], in that it introduces a set of parameters that provide control authority over the "exit" conditions from stance and flight. The power of the method is illustrated by considering a minimalist actuator setting, in which the three DOF ASLIP is controlled by a single actuator located at the hip. Such generalizations of the SLIP embedding controller can be extended in a straightforward fashion to control more complete than the ASLIP models of robots such as Thumper, as has been shown in [8].

Acknowledgment

The author wishes to thank J. W. Grizzle for inspiring discussions and for pointing [2], and. J. Hurst for Fig. 1(a).

References

[1] O. Arslan, U. Saranli, and O. Morgul, "An approximate stance map of the spring mass hopper with gravity correction for nonsymmetric locomotions," in *Proceedings of the IEEE International Conference of Robotics and Automation*, Kobe, Japan, May 2009, pp. 2388–2393.

[2] M. D. Di Benedetto and J. W. Grizzle, "Asymptotic model matching for nonlinear systems," *IEEE Transactions on Automatic Control*, vol. 39, no. 8, pp. 1539–1550, 1994.

[3] P. Holmes, R. J. Full, D. Koditschek, and J. Guckenheimer, "The dynamics of legged locomotion: Models, analyses, and challenges," *SIAM Review*, vol. 48, no. 2, pp. 207–304, May 2006.

[4] J. W. Hurst, "The role and implementation of compliance in legged locomotion," Ph.D. dissertation, The Robotics Institute, Carnegie Mellon University, 2008.

[5] S.-H. Hyon and T. Emura, "Symmetric walking control: Invariance and global stability," in *Proceedings of the IEEE International Conference on Robotics and Automation*, Barcelona, Spain, 2005, pp. 1455–1462.

[6] F. Iida and R. Tedrake, "Motor control optimization of compliant one-legged locomotion in rough terrain," in *Proceedings of the IEEE/RSJ International Conference on Intelligent Robots and Systems (IROS)*, San Diego, CA, USA, Nov. 2007, pp. 2230–2235.

[7] A. Isidori, *Nonlinear Control Systems*, 3rd ed. Berlin: Springer-Verlag, 1995.

[8] I. Poulakakis and J. W. Grizzle, "Modeling and control of the monopedal running robot Thumper," in *Proceedings of the IEEE International Conference on Robotics and Automation*, Kobe, Japan, 2009, pp. 3327–3334.

[9] ——, "The spring loaded inverted pendulum as the hybrid zero dynamics of an asymmetric hopper," *IEEE Transactions on Automatic Control*, vol. 54, no. 8, pp. 1779–1793, Aug. 2009.

[10] M. H. Raibert, *Legged Robots that Balance*. Cambridge, MA: MIT Press, 1986.

[11] U. Saranli, W. Schwind, and D. E. Koditschek, "Toward the control of a multi-jointed, monoped runner," in *Proceedings of the IEEE International Conference on Robotics and Automation*, vol. 3, Leuven, Belgium, May 1998, pp. 2676–2682.

[12] E. R. Westervelt, J. W. Grizzle, C. Chevallereau, J. H. Choi, and B. Morris, *Feedback Control of Dynamic Bipedal Robot Locomotion*. Taylor & Francis/CRC Press, 2007.